Melt Procedure Affects the Photosynthetic Response of Sea Ice Algae

Karley Campbell[1]*, C. J. Mundy[2], Andrew R. Juhl[3], Laura A. Dalman[2], Christine Michel[2,4], Ryan J. Galley[2], Brent E. Else[5], Nicolas X. Geilfus[2] and Søren Rysgaard[2,6,7]

[1] Bristol Glaciology Centre, University of Bristol, Bristol, United Kingdom, [2] Centre for Earth Observation Science, University of Manitoba, Winnipeg, MB, Canada, [3] Lamont-Doherty Earth Observatory, Columbia University, Palisades, NY, United States, [4] Fisheries and Oceans Canada, University Crescent, Winnipeg, MB, Canada, [5] Department of Geography, University of Calgary, Calgary, AB, Canada, [6] Arctic Research Centre, Department of Bioscience, University of Aarhus, Aarhus, Denmark, [7] Greenland Institute of Natural Resources, Nuuk, Greenland

The accuracy of sea ice algal production estimates is influenced by the range of melting procedures used in studies to obtain a liquid sample for incubation, particularly in relation to the duration of melt and the approach to buffering for osmotic shock. In this research, ice algal photophysiology from ^{14}C incubations was compared in field samples prepared by three melt procedures: (i) a rapid $\leq$ 4 h melt of the bottommost (< 1 cm) ice algal layer scraped into a large volume of filtered seawater (salinity 27–30), (ii) melt of a bottom 5 cm section diluted into a moderate volume of filtered seawater over 24 h (salinity 20–24), and (iii) melt of a bottom 5 cm section without any filtered seawater dilution over about 48 h (salinity 10–12). Maximum photosynthetic rate, photosynthetic efficiency and production at zero irradiance were significantly affected by the melt treatment employed in experiments. All variables were greatest in the highly diluted scrape sample and lowest in the bulk-ice samples melted in the absence of filtered seawater. Laboratory experiments exposing cultures of the common sea ice diatom *Nitzschia frigida* to different salinities and light conditions suggested that the field-based responses can be attributed to the rapid (< 4 h) adverse effects of exposing cells to low salinities during melt without dilution. The observed differences in primary production between melt treatments were estimated to account for over 60% of the variability in production estimates reported for the Arctic. Future studies are strongly encouraged to replicate salinity conditions representative of *in situ* values during the melting process to minimize hypoosmotic stress, thereby most accurately estimating primary production.

Keywords: sea ice, algae, salinity stress, photophysiology, sample melt, Arctic

INTRODUCTION

Algae colonizing the brine network and bottom layer of sea ice are estimated to account for 3–25% of annual primary production in the Arctic Ocean (Subba Rao and Platt, 1984; Legendre et al., 1992), although greater contributions have been documented in high Arctic regions (Gosselin et al., 1997). In particular, a bloom of largely photosynthetic diatoms in spring provides a concentrated

food resource for aquatic grazers (Leu et al., 2011), which also influences the flux of CO_2 between the atmosphere and ocean (Brown et al., 2015). The availability of light and nutrients are understood to be important controls of ice algal abundance and productivity (Leu et al., 2015), but the magnitude of variability in production estimates reported across the Arctic, even between studies of seemingly comparable environments, requires further investigation (Leeuwe et al., 2018). There are renewed efforts to expand the spatial coverage of sea ice production measurements as recent studies have shown that ice algae in previously under sampled regions may be greatly underestimated (Lange et al., 2017; Fernandez-Mendez et al., 2018). Timely completion of such assessments of sea ice algal communities are required to predict the consequences of climate warming on ice algae, including the impact of ongoing changes to sea ice volume, seasonality and areal coverage (Vihma, 2014; Simmonds, 2015).
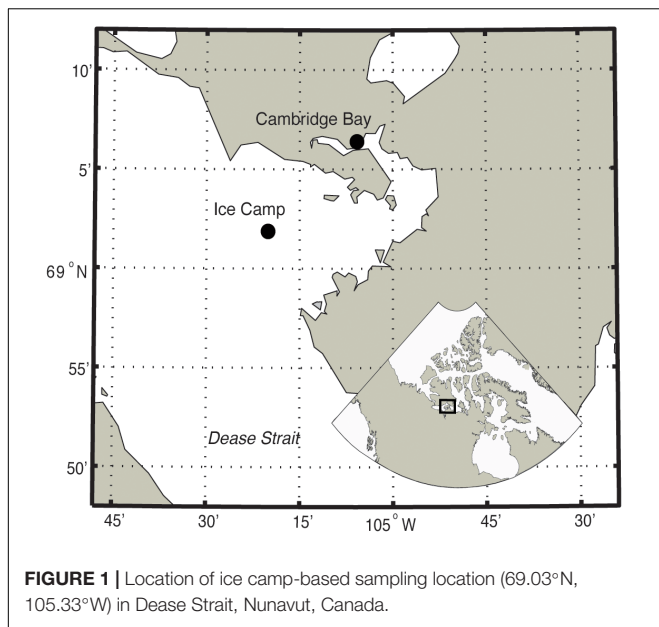
Effective studies of sea ice biogeochemistry rely on accurate measurements of ice algal production, which can be done by monitoring oxygen evolution or carbon uptake *in situ* or via incubation of samples in a closed system. *In situ* approaches, such as quantifying oxygen flux across the ocean-ice diffusive boundary layer (McMinn et al., 2000; Rysgaard et al., 2001; McMinn and Hegseth, 2007), arguably provide estimates under the most natural conditions. However, these methods can be costly, time consuming, and dangerous if divers are required for the deployment of sensors (Bates and Cota, 1986). Furthermore, the corresponding biomass, areal footprint, as well as the role of physical processes (e.g., ice melt) on flux measurements is often uncertain (Kuhl et al., 2001). There are also concerns related to gas and tracer diffusion when measuring algal production within the solid ice matrix (Mock and Gradinger, 1999).

For these reasons, sea ice productivity studies typically use melted sections of sea ice cores (Leeuwe et al., 2018) or, to a lesser extent, sea ice brine (McMinn et al., 2014). Incorporation of liquid samples into specialized incubators further permits a range of assessments, such as construction of photosynthesis-irradiance (PE) curves to assess algal photophysiology (Cota and Horne, 1989) that have been widely used in studies of sea ice algal production across the Arctic (e.g., Michel et al., 1988; Bergmann et al., 1991; Søgaard et al., 2010; Campbell et al., 2016). It is more common to incubate melted bulk-ice samples than collecting sea ice brine because all cells, independent of size, are obtained from a known section of an ice core (Norrman and Anderson, 1994). This is also a practical approach when studying the Arctic spring bloom given that sea ice algae are predominantly concentrated in the bottommost skeletal layer of first-year ice during this time (Leu et al., 2015). Furthermore, sampling the growth interface rather than the brine network collects the majority of biomass for subsequent analysis. Despite widespread measurement of primary productivity on melted ice samples, there is a lack of consensus in the scientific community on the specific melt procedure to employ (Miller et al., 2015). Samples are consistently melted in darkness to avoid light stress on the shade acclimated algae; however, approaches vary in the temperature and duration of melt used, as well as whether the sample is buffered for the decrease in salinity that occurs with melting of the solid ice matrix.

Carbon-fixation of ice algal communities is greatest between 4 and 14°C (Kottmeier and Sullivan, 1988; Arrigo and Sullivan, 1992), which is significantly warmer than the subzero temperatures experienced by cells in the ice environment. Ice algae are thus capable of functioning over a wide range of temperatures. However, recent assessments of sea ice sample melt temperatures have shown conflicting results, likely due to the inherent link between temperature and duration of melt. For example, Rintala et al. (2014) demonstrated no significant difference in algal productivity between samples melted at room temperature (~12 h) or at 4°C (36 h) and advocated for a rapid melt to limit the influence of biological impacts (e.g., growth of algae and bacteria) that are likely to increase over time. In contrast, Mikkelson and Witkowski (2010) showed that melting over approximately 14 h at room temperature (20°C) caused significantly lower abundances of non-diatom cells that often dominate ice communities outside of the bloom period, concluding that rapid melt at temperatures warmer than 4°C should be avoided.

Sea ice algae have the capacity to survive a broad range of salinities, with maximum photosynthetic rates typically found at salinities comparable to ocean surface water (Grant and Horner, 1976; Kottmeier and Sullivan, 1988). Nevertheless, studies have shown that sea ice algae are susceptible to osmotic shock, particularly if not given sufficient time to gradually acclimate to decreasing salinity (Kirst, 1990; Ryan et al., 2004). This can include damage to cell pigments and the potential release of intracellular carbon and nutrient pools, although the impact on diatoms is thought to be less than algae of other functional groups (Kirst, 1990).

To avoid the potential effects of hypoosmotic shock, adding filtered seawater at about 3–4 times the volume of ice collected has been encouraged by a number of studies to buffer salinity during the melting process (Garrison and Buck, 1986; Ryan et al., 2004; Mikkelson and Witkowski, 2010; Thomas et al., 2010; Campbell et al., 2018). Still others have employed higher-dilution methods, like the 'scrape' sampling approach that melts the bottommost skeletal layer into much greater volumes of seawater (Smith et al., 1988; Cota and Horne, 1989; Bergmann et al., 1991), or diver-operated suction-type samplers (Welch et al., 1988) that collect algal cells from the ice-ocean interface and ice bottom in a mix of ambient (unfiltered) interface and brine water (Welch and Bergmann, 1989; Gosselin et al., 1990, 1997; Johnsen and Hegseth, 1991; Hegseth, 1998). One potential drawback of adding filtered seawater during the melting process is that it may introduce additional constituents which artificially enhance photosynthesis (Rintala et al., 2014), though these external inputs are likely to be insignificant relative to intracellular pools of nutrients unless standing stocks are high (Thomas et al., 2010). As a result, a number of studies on sea ice communities have melted ice samples without buffering for salinity (e.g., Kaartokallio et al., 2007; Søgaard et al., 2010; Fernandez-Mendez et al., 2018). Conflicting recommendations for melting sea ice have resulted in the use of different approaches in different studies. The array of techniques employed raises concerns regarding the accuracy of measurements relative to *in situ* communities and may contribute to variability in

FIGURE 1 | Location of ice camp-based sampling location (69.03°N, 105.33°W) in Dease Strait, Nunavut, Canada.

production estimates across polar regions (Arrigo et al., 1997; Leeuwe et al., 2018).

The main objective of this study was to investigate how different sample melting procedures may impact subsequent measurements of primary productivity. First, we conducted field-based experiments to test the hypothesis that melt procedure had a significant impact on the productivity and photophysiology of sea ice algae in Dease Strait of the Canadian Arctic Archipelago. We then conducted laboratory experiments on cultures of the prevalent ice diatom species *Nitzschia frigida* to investigate the relative importance of conditions that cells experience during different melt procedures. Based on the results of these experiments we provide recommendations for melt procedure in future studies of sea ice algal photophysiology.

MATERIALS AND METHODS

Collection and Processing of Dease Strait Samples

Site Characteristics and Description of Field-Based Melt Treatments

Field data were collected from the first-year sea ice in Dease Strait, Canada, on five occasions between 17 May and 9 June 2014 (**Figure 1**). Areas of thin snow cover (< 10 cm) were selected for sampling approximately every 4 days in this region. During four of the five sampling events a scrape melt treatment was obtained by collecting the bottom $\sim$1 cm of six ice cores using a Mark II Kovacs core barrel. These scrape samples were pooled by placing scrapes directly into filtered seawater (FSW), for a dilution factor of approximately eight. Total volume of FSW and scrape samples was not measured directly and was instead estimated assuming that 1 cm of ice was collected per core (FSW$_{8:1}$). On each date of sample collection, the bottom

5 cm of 12–16 different cores were also collected and core segments were split into two separate insulated containers before transport back to the field laboratory for processing under two other melt treatments that included: (i) diluted melt with filtered seawater added at a volumetric ratio of three parts filtered seawater to one part ice (FSW$_{3:1}$), and (ii) undiluted melt without the addition of filtered seawater (FSW$_{zero}$). With each replicate representing an individual sampling event, the result is a total of four sample replicates for FSW$_{8:1}$ scrapes and five replicates for FSW$_{3:1}$ and FSW$_{zero}$ melt treatments. All filtered seawater was collected from 2.5 m depth 24–48 h prior to ice collection using a Kemmerer sampler deployed through the ice and was prepared at room temperature using 0.2 μm polycarbonate filters. Filtered seawater added to ice for melt was also at room temperature. Melting of all samples took place within the insulated containers that were stored in a dark room at approximately 20°C. Samples were periodically checked for complete ice melt, about 4 h for FSW$_{8:1}$, 24 h for FSW$_{3:1}$, and 48 h for FSW$_{zero}$. Samples were analyzed as soon as possible (within $\sim$1 h) after complete melt to prevent significant warming above the melting point of sea ice in containers. These melt treatments of pooled cores for each sampling event were used for all field-based measurements presented.

Sampling of Biological and Chemical Variables in Dease Strait

Chlorophyll *a* concentration (chl *a*) was determined by filtering two subsamples from each of the three melted core treatments onto GF/F filters (Whatman), and measuring fluorescence (Turner Designs Trilogy Fluorometer) of pigments extracted into 10 ml of 90% acetone for 18–24 h before and after acidification with 5% HCl (Holm-Hansen et al., 1965; Parsons et al., 1984). The resultant concentrations of chl *a* reported were further corrected for melt dilution. Salinity of each melted ice sample was measured using an Orion Star A212 conductivity meter upon complete melt. On average ($\pm$ SD) the salinity of FSW$_{8:1}$, FSW$_{3:1}$, and FSW$_{zero}$ samples were 27.0 $\pm$ 0.2, 24.1 $\pm$ 0.3, 9.6 $\pm$ 1.1, respectively. The salinity of melted ice samples was proportional to volume of seawater added, where the salinity of filtered seawater averaged 28.3 $\pm$ 0.4 during the sampling period.

During each coring event, the bottom 5 cm of a separate ice core (melted without dilution at room temperature in the dark) and water sample collected from the base of a cored hole via submersible pump, were taken to measure nutrients in the bottom-ice and at the ice-ocean interface, respectively. Filtered seawater collected for melt treatments was also subsampled for nutrients within 24–48 h of collection. Nutrient samples were processed using acid sterilized syringes (HCl) and GF/F filters (Whatman) previously combusted at 450°C for 5 h. Filtrate was frozen at –20°C prior to analysis of nitrate (NO$_3$) and nitrite (NO$_2$), phosphate (PO$_4$) and silicic acid (Si(OH)$_4$) concentrations using a Seal Analytical auto analyzer within 6 months of collection (Grasshoff et al., 1983).

Pseudo-duplicate samples of the melted bulk-sea ice, filtered seawater and interface water were collected in 12-ml Exetainers and fixed with 20 μl of saturated mercury chloride (HgCl$_2$) solution for later analysis of dissolved inorganic carbon (DIC).

Average DIC concentration was measured within 6 months of sample collection using an Apollo Scitech Inc. infrared CO_2 analyzer. Routine analysis of Certified Reference Materials provided by A. G. Dickson, Scripps Institution of Oceanography, verified that DIC were analyzed within $\pm 3\,\mu mol\,kg^{-1}$.

Measurement of Gross Primary Production on Field Samples

Photosynthesis-irradiance curves of gross primary production relative to chl a were calculated for each of the melt treatments using the ^{14}C tracer method (Strickland and Parsons, 1972). This consisted of incubating subsamples of pooled cores in 60 ml polystyrene culture flasks (Corning) over a range of 10 different light intensities from 8 to 200 $\mu mols\,m^2\,s^{-1}$, and in two dark bottles that were spiked with 50 μl of 3-3,4-dichlorophenyl-1,1-dimethylurea (DCMU; Legendre et al., 1983). Once inoculated with 1 ml of ^{14}C (4 $\mu Ci\,ml^{-1}$), for a final concentration of $\sim 0.07\,\mu Ci\,ml^{-1}$ per culture flask, samples were incubated in chambers modeled after Babin et al. (1994) for 3 h at $-1.5°C$ to represent approximate *in situ* temperatures. During this time, chambers were placed on a shaker table to promote cell suspension, while also being illuminated by a full spectrum halogen lamp (Phillips Ceramalux). The average light intensity (n = 3) at each bottle position was determined prior to incubations by measuring integrated photosynthetically active radiation (PAR) (μmol photons $m^{-2}\,s^{-1}$) using a scalar PAR probe (Walz model US-SQS/L) and data logger (LI-COR LI-1000) in a water-filled incubation flask, while keeping surrounding sample-filled flasks in place. Incubations of photosynthesis-irradiance curves were typically started ± 2 h of 1300 local time.

Following incubation, samples were filtered onto 25 mm GF/F filters (Whatman), placed into 7 ml glass scintillation vials, and acidified with 200 μl 0.5 N HCl to remove any unfixed carbon. Once dry, 5 ml of Ecolume scintillation cocktail was added to each vial, followed by an extraction period of 24–48 h before measurement of activity on a Hidex Triathler liquid scintillation counter. Initial ^{14}C activity was determined from the average of 3–50 μl aliquots of spiked sample that had been randomly removed from clear flasks prior to the start of incubation. These samples were placed into a solution of 5 ml scintillation cocktail and 50 μl ethanolamine (to prevent degassing) for extraction prior to counting. Gross primary productivity of ^{14}C incubations was calculated from scintillation counts, initial ^{14}C activity, and DIC concentrations (see Section "Sampling of biological and chemical variables in Dease Strait") of sample melt following the equation of potential primary productivity outlined in Søgaard et al. (2010).

Photosynthesis-irradiance curves were modeled using an exponential function in the absence of photoinhibition (Platt et al., 1980; Arrigo et al., 2010), as it was not observed, to determine photophysiological parameters that include: maximum photosynthetic rate, P^B_s (mg C mg chl $a^{-1}\,h^{-1}$), photosynthetic efficiency, α^B (mg C mg chl $a^{-1}\,h^{-1}$ (μmol photons $m^{-2}\,s^{-1})^{-1}$)), production at zero irradiance, P_0 (mg C mg chl $a^{-1}\,h^{-1}$), the compensation point, E_c (μmol photons $m^{-2}\,s^{-1}$) and the photoacclimation index, E_s (μmol photons $m^{-2}\,s^{-1}$) (Cota and Smith, 1991; Arrigo et al., 2010).
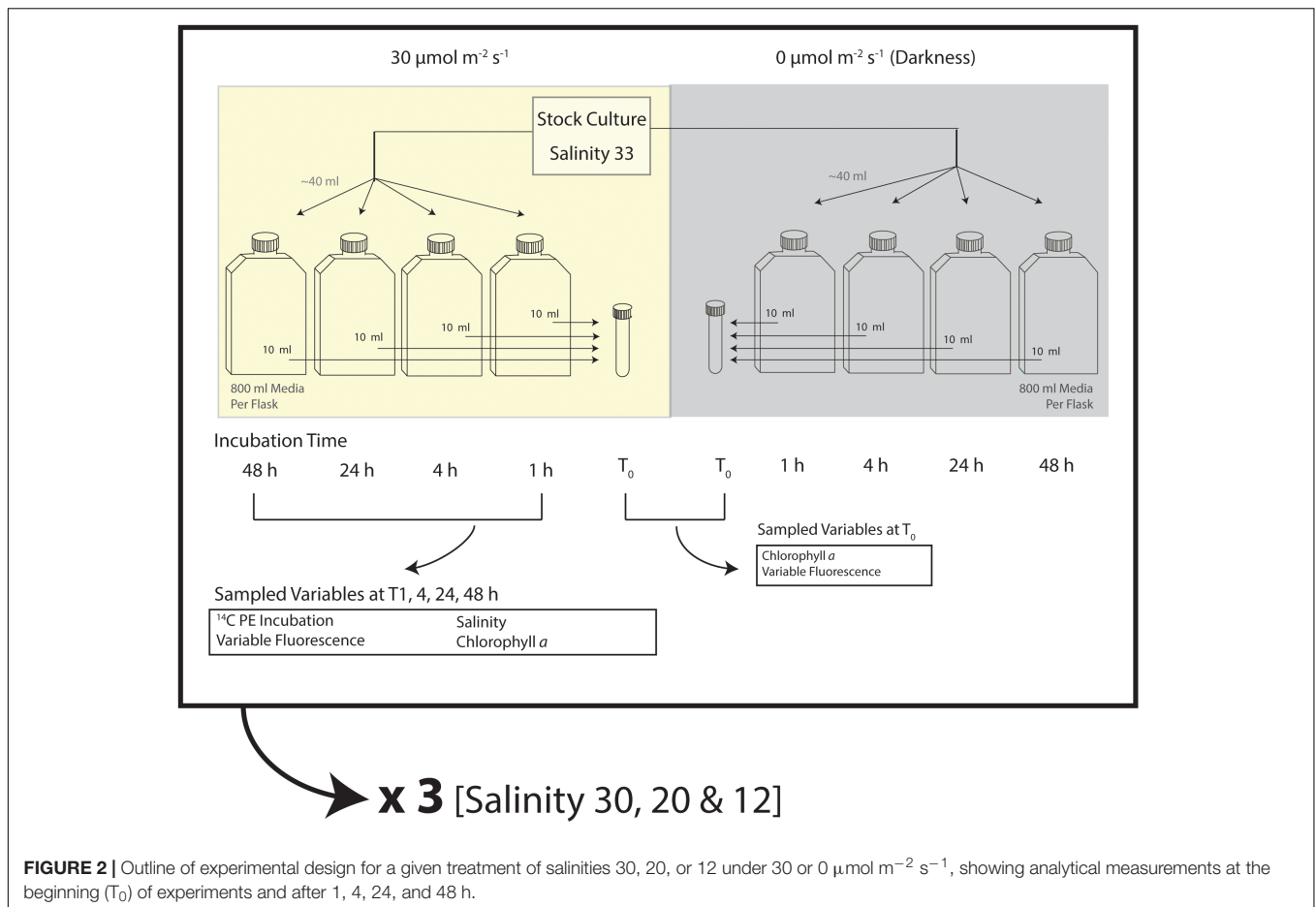
Laboratory-Based Culture Experiments
Growth and Preparation of Diatom Cultures
The large differences in several photophysiological parameters observed between the three melt treatments applied to field samples appeared to be related to the relative change in salinity experienced by ice algae during each melt procedure. To support this hypothesis, lab experiments were designed to test whether salinity changes comparable to those that occurred during the different melt procedures (or the change in salinity plus darkness) could by themselves produce photophysiological changes in ice algae of comparable magnitude to those observed in the field samples. Because the three melt procedures also vary in their duration, the experiments assessed the potential for temporal changes in photophysiological parameters during exposure of cells to low salinity and darkness over 48 h.

The pennate diatom species *N. frigida* was selected for these experiments due to its known abundance in spring ice algal communities across the Arctic (Różańska et al., 2009; Poulin et al., 2011), including in the region of Dease Strait where species of *Nitzschia* comprised 24% and *N. frigida* 10% of the algal community between 17 May and 5 June 2014 (Campbell et al., 2018). Cultures of *N. frigida* originally isolated from landfast sea ice of the nearshore Chukchi Sea (Aumack and Juhl, 2015), were transferred to the University of Manitoba for experiments. Stock and experimental cultures were grown in sterile L1 medium (Guillard and Hargraves, 1993) made using artificial seawater (Instant Ocean). When grown at 1°C in media with a salinity of 33 and exposure to photosynthetically active radiation of 30 $\mu mol\,m^{-2}\,s^{-1}$, exponential phase growth rates of approximately 0.4 d^{-1} were comparable to others of *N. frigida* under similar conditions (Suzuki et al., 1997; Juhl and Krembs, 2010).

Procedure for Experimentation on Diatom Cultures
Experiments tested the photophysiological responses of *N. frigida* to salinities similar to the three field-based melt treatments ($FSW_{8:1}$, $FSW_{3:1}$, and FSW_{zero}), under near growth saturating light and darkness. L1 media of three different salinities comparable to the three field-based melt treatments (30, 20, and 12, respectively) were created by modifying the amount of Instant Ocean dissolved to make the artificial seawater base. The resultant experimental treatments at salinity 30, 20, and 12 are hereafter referred to as S30, S20, and S12, respectively. Initial nutrient, trace metal and vitamin concentrations were consistent for all salinities. For a given salinity treatment, 40 ml of stock *N. frigida* were transferred into each of eight-1 L polystyrene culture flasks (Thermo Scientific) containing 800 ml of experimental L1 growth media, previously cooled to 1°C (**Figure 2**). Samples were gently mixed and then 10 ml of inoculated media from each of the 8 flasks were pooled to provide an average initial (T_0) sample. Flasks were then sealed and placed into one of the two light conditions (30 or 0 μmol photons $m^{-2}\,s^{-1}$, n = 4 for each light treatment) in a 1°C incubator. Thirty μmol photons $m^{-2}\,s^{-1}$ was expected to result in nearly maximal growth rate in *N. frigida* (Suzuki et al., 1997; Juhl and Krembs, 2010). To assess the

FIGURE 2 | Outline of experimental design for a given treatment of salinities 30, 20, or 12 under 30 or 0 μmol m^{-2} s^{-1}, showing analytical measurements at the beginning (T$_0$) of experiments and after 1, 4, 24, and 48 h.

potential time-dependence of photophysiological responses, one flask from each combined salinity/light treatment was sacrificed for measurements (see Section "Analysis of data from culture experiments") at each designated time interval of 1, 4, 24, or 48 h. These time intervals were specifically chosen to assess short and long-term responses that correspond to field-based melt times of FSW$_{8:1}$ (4 h), FSW$_{3:1}$ (24 h), and FSW$_{zero}$ (48 h) samples. The result was measurements of photophysiology in 48 flasks in a given experimental run, with each flask representing a single treatment combination of salinity, light and time. Two experimental runs were completed, providing duplicate measurements for each treatment combination.

Analysis of Data From Culture Experiments

Experimental samples of T$_0$ and time intervals 1, 4, 24, and 48 h were processed immediately after removal from the incubator for maximum quantum efficiency of PSII, chl *a* and salinity (**Figure 2**). A total of five measurements of *in vivo* fluorescence were first measured on each of the duplicate-5 ml subsamples taken from each melt treatment flask (Turner Designs Trilogy Fluorometer), before (F$_0$) and after (F$_m$) 20 μl DCMU (< 0.1%) was added to induce maximum fluorescence. Each sample was gently mixed to suspend cells in solution prior to *in vivo* fluorescence measurements. The maximum quantum yield of

photosystem II (Fv/Fm) was calculated as $[(F_m - F_0)/F_m]$ (Maxwell and Johnson, 2000; Parkhill et al., 2001), and is reported hereafter as a combined average of duplicate Fv/Fm measurements for the two experimental runs. Chlorophyll *a* and salinity were measured following the protocols described previously, as was ^{14}C-derived primary production that was measured on samples from time intervals 1, 4, 24, and 48 h (**Figure 2**). Since DIC could not be directly measured for the experimental solutions, the concentration of DIC used to calculate primary production was based on experimental temperature and salinity, assuming 100% saturation (Parsons et al., 1984).

Statistical Analyses for Field and Laboratory-Based Results

Matlab (R2016a) was used for fitting of all exponential photosynthesis-irradiance curves. SPSS statistical software (IBM Version 20) was used for all statistical analyses. When comparing photophysiological parameters of the three field-based melt procedures, one-way ANOVA was performed with Fisher's *post hoc* test. Parametric linear regression was used to test for temporal trends in experimental results. Photophysiological data found to be not normally distributed by a Shapiro–Wilk test or have inhomogeneous variances via Levene test were first log transformed prior to statistical analyses, but are otherwise

reported as original values with units defined in the text. ANOVA results are reported with the F statistic (F(df_1, df_2), where df_1 is the degrees of freedom for melt treatments and df_2 is the number of observations less the number of melt treatments, overall p-value for the model, as well as the p-values for the respective *post hoc* tests. Regression results are reported with the r^2 and p-value. Significance of statistical analyses in this research was concluded for $p < 0.05$ for a given test unless otherwise specified.

RESULTS

Sea Ice Experiments of Dease Strait
Biological and Chemical Characteristics of the Sampling Location

The physical and biological characteristics of sites in Dease Strait sampled from 17 May to 9 June 2014 are summarized in **Table 1**. Selection of thin snow cover resulted in a relatively constant snow and ice thickness throughout the sample period. Stable ice thickness combined with observations of low bulk-ice salinity and bottom-ice (5 cm) temperatures around the $-1.5°C$ freezing point of seawater at salinity 28 also indicate that sampling took place near the onset of spring melt. Average $NO_2 + NO_3$ concentrations in the bottom-ice and water immediately below the sea ice were low, generally less than 1 μmol L^{-1}. The ice algal community was largely comprised of *Attheya* and *Nitzschia* diatom species, which over a given 24 h day, were exposed to light intensities averaging 29 μmol m^{-2} s^{-1} during our study period (Campbell et al., 2016).

TABLE 1 | Average values with standard deviation (brackets) for environmental and oceanographic parameters at the study location in Dease Strait, sampled between 17 May and 9 June ($n = 5$).

	Parameter	Average (SD)
General	Snow thickness (cm)	9.40 ± 5.15
	Ice thickness (cm)	197.7 ± 3.86
	Transmitted irradiance (μmol m^{-2} s^{-1}) [Campbell et al., 2017]	28.8 ± 7.87
Filtered seawater	DIC (μmol kg^1)	2000 ± 30
	Salinity	28.3 ± 0.4
	$NO_2 + NO_3$ (μmol L^{-1})	0.25 ± 0.29
	PO_4 (μmol L^{-1})	1.07 ± 0.24
	$Si(OH)_4$ (μmol L^{-1})	6.40 ± 1.30
Bulk-ice	Temperature (°C)	−1.44 ± 0.15
	Salinity	8.37 ± 0.76
	$NO_2 + NO_3$ (μmol L^{-1})	0.32 ± 0.07
	PO_4 (μmol L^{-1})	3.64 ± 1.41
	$Si(OH)_4$ (μmol L^{-1})	2.68 ± 0.93
Sea ice-Ocean Interface	Salinity	28.2 ± 0.13
	$NO_2 + NO_3$ (μmol L^{-1})	0.94 ± 0.14
	PO_4 (μmol L^{-1})	0.90 ± 0.04
	$Si(OH)_4$ (μmol L^{-1})	5.42 ± 0.38

Field-Based Melt Treatments

Salinity and DIC concentration were greatest in the $FSW_{8:1}$ melt treatment, followed by the $FSW_{3:1}$ and FSW_{zero} treatments (**Supplementary Table S1**). The salinity and DIC of the highly diluted $FSW_{8:1}$ treatment were most similar to concentrations measured in filtered seawater that had an average salinity of 28.3 ± 0.4 and DIC concentration of 2000 ± 30 μmol kg^1. Inorganic nutrient content of the filtered seawater has been summarized in **Table 1**.

Primary production at a given light level was consistently highest in the $FSW_{8:1}$ samples, followed by $FSW_{3:1}$ and FSW_{zero} samples, respectively (**Figure 3A**). This is highlighted by significantly different P^B_s, α^B, and P_0 between FSW_{zero} and all other melt treatments, which were greatest in $FSW_{8:1}$ and lowest in FSW_{zero} melt treatments. Photophysiological parameters E_c and E_s were not significantly different between melt treatments (**Table 2**). Modeled production for $FSW_{3:1}$ on 14 June did not intercept the x-axis at zero irradiance, and as a result, P_0 and E_c were not calculated for this sample date.

Laboratory Experiments on *Nitzschia frigida* Cultures

Lab experiments were run to determine whether changes in salinity alone, or salinity with darkness, could produce changes in photophysiology that were comparable to those observed in field samples under the different melt conditions (**Figure 3**).

Chlorophyll *a* and Maximum Quantum Efficiency of PSII of Cultures

Conditions of laboratory experiments on *N. frigida* cultures are summarized in **Supplementary Table S2**. The concentration of chl *a* in treatments ranged between 17.5 and 52.0 μg L^{-1} (**Figure 4A**) and exhibited no apparent relationship with salinity treatment or light condition. The concentration of chl *a* increased over the duration of experiments in S30 and S20 samples exposed to 30 μmol m^{-2} s^{-1}, but decreased over time at S12 under illuminated or dark conditions (**Figure 4A**). The maximum quantum efficiency of PSII of S12 samples under light or dark conditions were lower than S30 and S20 salinity treatments, respectively (**Figure 4B**). At S30 and S20, Fv/Fm of light and dark samples appeared to increasingly deviate over incubation time, with fluorescence at 30 μmol following similar trends as chl *a* described previously (**Figure 4B**).

Photosynthesis-Irradiance (PE) Curves of Salinity Treatments in Culture Experiments

Photophysiological parameters P^B_s, α^B and P_0 within each experimental light condition (i.e., light or dark) were highest at S30, followed by S20 and S12, respectively (**Figures 3B, 5**). Parameters P^B_s, α^B, and P_0 at S12 showed the greatest differences in responses between light and dark conditions (**Supplementary Table S3**). In comparison, the response of E_c and E_s was similar for algae grown in the three melt treatments; although, average measurements were consistently lower in dark versus light conditions (**Supplementary Table S3**). The majority of photophysiological parameters showed no significant temporal
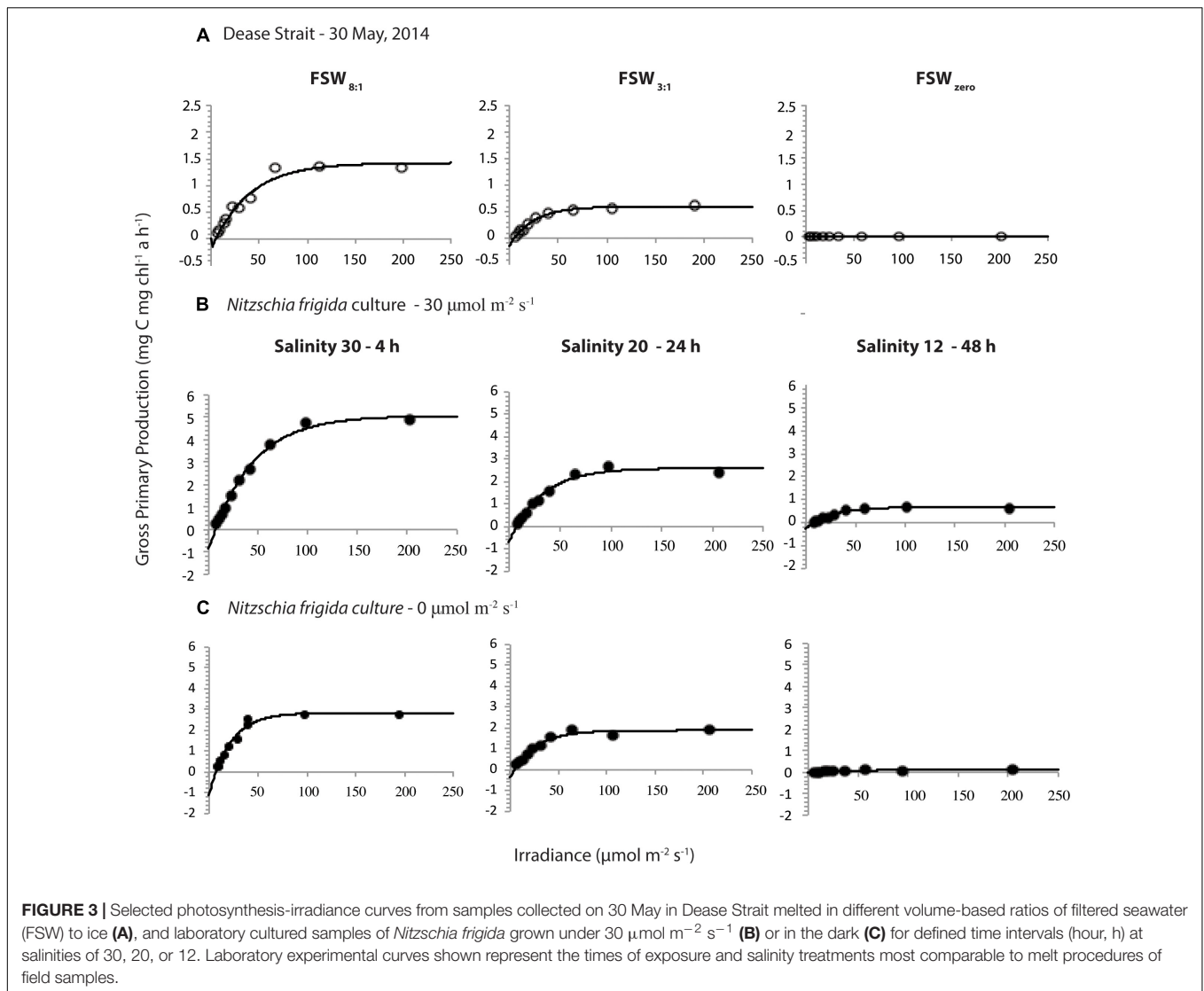
FIGURE 3 | Selected photosynthesis-irradiance curves from samples collected on 30 May in Dease Strait melted in different volume-based ratios of filtered seawater (FSW) to ice **(A)**, and laboratory cultured samples of *Nitzschia frigida* grown under 30 μmol m^{-2} s^{-1} **(B)** or in the dark **(C)** for defined time intervals (hour, h) at salinities of 30, 20, or 12. Laboratory experimental curves shown represent the times of exposure and salinity treatments most comparable to melt procedures of field samples.
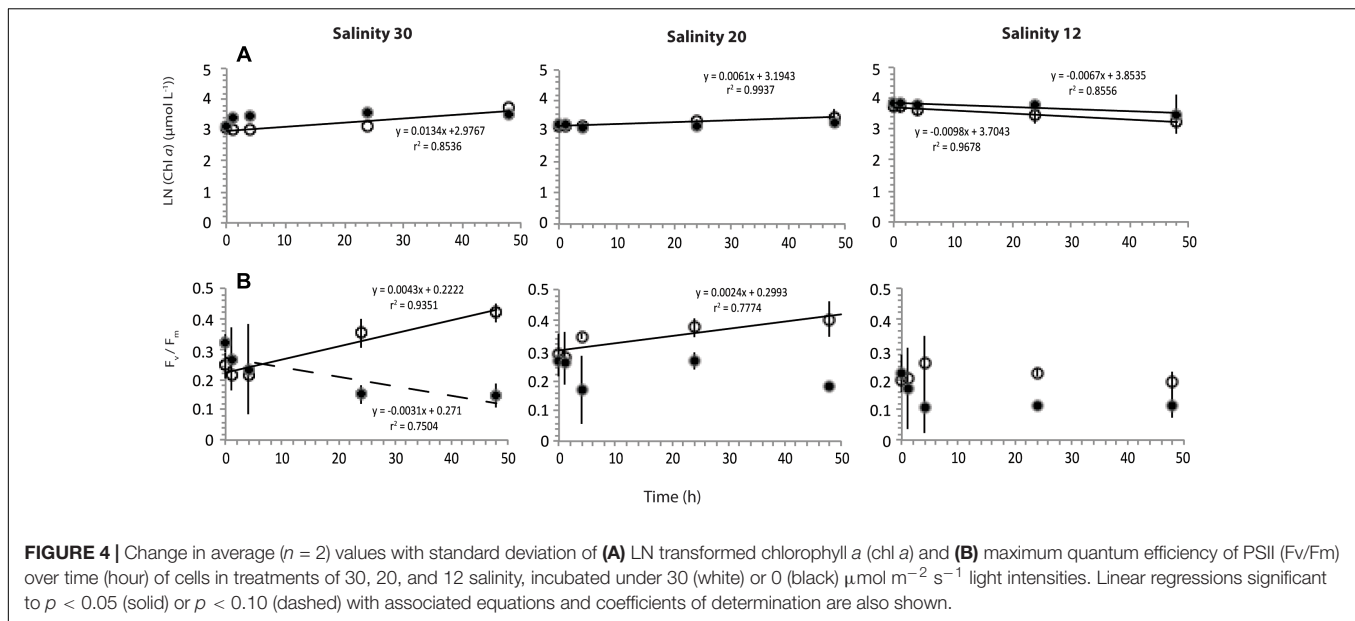
TABLE 2 | Average values with standard deviation (brackets) of photosynthesis-irradiance parameters (see text for definitions) for samples melted in filtered sea water added at a ratio of eight parts water to one part ice (FSW$_{8:1}$), three parts water to one part ice (FSW$_{3:1}$), and melted without filtered seawater added (FSW$_{zero}$).

		Average			ANOVA	Fisher's *post hoc* test of significance		
		FSW$_{8:1}$	FSW$_{3:1}$	FSW$_{zero}$	F Statistic *p*-value (df)	FSW$_{8:1}$ vs. FSW$_{3:1}$	FSW$_{8:1}$ vs. FSW$_{zero}$	FSW$_{3:1}$ vs. FSW$_{zero}$
PE Parameters	P^B_s	2.03 (0.661)	0.762 (0.121)	0.077 (0.112)	**34.730 <0.001 (2, 11)**	0.108	**<0.001**	**<0.001**
	α^B	0.062 (0.021)	0.024 (0.005)	0.004 (0.007)	**18.741 <0.001 (2, 11)**	0.147	**0.001**	**<0.001**
	P$_0$	0.295 (0.132)	0.097 (0.043)	0.016 (0.026)	**16.378 0.001 (2, 10)**	0.158	**0.003**	**<0.001**
	E$_c$	4.63 (0.735)	2.80 (2.56)	4.59 (1.28)	0.681 0.528 (2, 10)	0.306	0.365	0.854
	E$_s$	33.4 (5.29)	40.8 (20.5)	32.1 (18.0)	0.532 0.602 (2, 11)	0.670	0.325	0.604

The ANOVA test statistic F (top), p-value (bottom), and Fisher's post hoc p-value are presented. Significant values (p < 0.05) are in bold. Degrees of freedom (df) in the ANOVA model is also shown.

trends between hour 1 and 48 of the experiments, with the exception of increases of illuminated sample P^B_S at S12 ($r^2 = 0.988$), P$_0$ at S12 ($r^2 = 0.917$), and E$_c$ at S30 ($r^2 = 0.928$), as well as α^B of darkened samples at S20 ($r^2 = 0.461$) (**Figure 5**).

Nevertheless, we note that in many instances (e.g., α^B at S30) the difference in P^B_s, α^B and P$_0$ parameters between individual time points of the experiment is greatest between hours 1 and 4, followed by more consistent values thereafter.

FIGURE 4 | Change in average ($n = 2$) values with standard deviation of **(A)** LN transformed chlorophyll a (chl a) and **(B)** maximum quantum efficiency of PSII (Fv/Fm) over time (hour) of cells in treatments of 30, 20, and 12 salinity, incubated under 30 (white) or 0 (black) μmol m^{-2} s^{-1} light intensities. Linear regressions significant to $p < 0.05$ (solid) or $p < 0.10$ (dashed) with associated equations and coefficients of determination are also shown.

DISCUSSION

Differences in the Physical Characteristics and Production of Algal Communities in Dease Strait Melt Treatments

Observations of higher chl a in FSW$_{8:1}$ than the other melt treatments (**Supplementary Table S1**), indicates that algal abundance likely increased toward the bottom-ice interface. That is, there is more algal pigment in the bottom 1 cm than the bottom 5 cm per liter of melted sea ice. Based on areal concentrations, chl a in the bottom 1 cm (FSW$_{8:1}$) of sea ice accounted for 145 ± 50 % of total chl a in the bottom 5 cm (FSW$_{zero}$) of sea ice during this study. Alternatively, if dilution corrected measurements of chl a in the bottom 1 cm of ice (FSW$_{8:1}$) are divided by five to simulate distributing the bottom 1 cm layer over a 5 cm core segment, the resultant average concentration ($115.0 \pm 14.1 \mu$g L^{-1}) would be similar to the chlorophyll values observed in the FSW$_{3:1}$ treatment (**Supplementary Table S1**). This agrees with previous observations that the majority of biomass in first-year sea ice is near the very bottom due to greater nutrient availability with proximity to interface water (Smith et al., 1990; McMinn et al., 1999), especially under relatively thin snow cover (Aumack et al., 2014). Thus the majority of algal chl a in this study was located in the bottom 0 to 1 cm section of ice, while negligible concentrations of chl a existed 1 to 4 cm from the ice-water interface.

The collection of a 1 cm scrape for the FSW$_{8:1}$ melt treatment versus 5 cm core sections for FSW$_{3:1}$ and FSW$_{zero}$ melt treatments introduces some uncertainty in the statistical comparison of field samples, as the different sections of sea ice could have contained physiologically unique communities. This includes potentially different algal species under greater nutrient stress with distance from the ocean-ice interface. However,

the overwhelming proportion of biomass in the 0 to 1 cm horizon would dominate the production signal and therefore, the effect of algal cells from 1 to 5 cm ice core section on the observed photophysiological parameters would be limited. Concentration of algae in the bottom centimeter of ice also supports that the three melt treatments in Dease Strait contained largely the same algal population, and thus their comparison may be used to highlight the collective response of the ice algal community to the conditions of sample melt. Finally, we note that the proportion of dominant pennate and centric functional groups was very similar between all three melt treatments (**Supplementary Table S4**), indicating that the melt treatments were likely of similar species composition.

Independent of this potential sampling bias, a difference of $> 50\%$ in chl a between FSW$_{3:1}$ and FSW$_{zero}$ samples from similar 0 to 5 cm core sections (**Supplementary Table S1**) reaffirms that the ice algal community was affected by the melt technique. Differences in P^B_s and α^B between the three melt treatments measured on Dease Strait samples further supports the important influence of melting procedure. In particular, values for P^B_s, α^B, and P$_0$ were consistently higher in the FSW$_{8:1}$ sample, followed by FSW$_{3:1}$ and FSW$_{zero}$, respectively (**Table 2**), illustrating that the magnitude of parameters likely increased with the proportion of filtered seawater added, or alternatively, decreased with the duration of ice melt. In comparison, differences in the E$_c$ and E$_s$ between melt treatments were not observed, suggesting these photophysiological parameters that characterize the light dependent mechanisms of photosynthesis are less sensitive to the stresses produced by melting. Similarly, sample melt did not appear to affect the composition of the ice algal community, as the proportion of pennate versus centric diatoms was relatively constant between melt treatments (**Supplementary Table S4**).

The results of this study largely contrast with those reported by Rintala et al. (2014) for sample of Baltic Sea ice, where
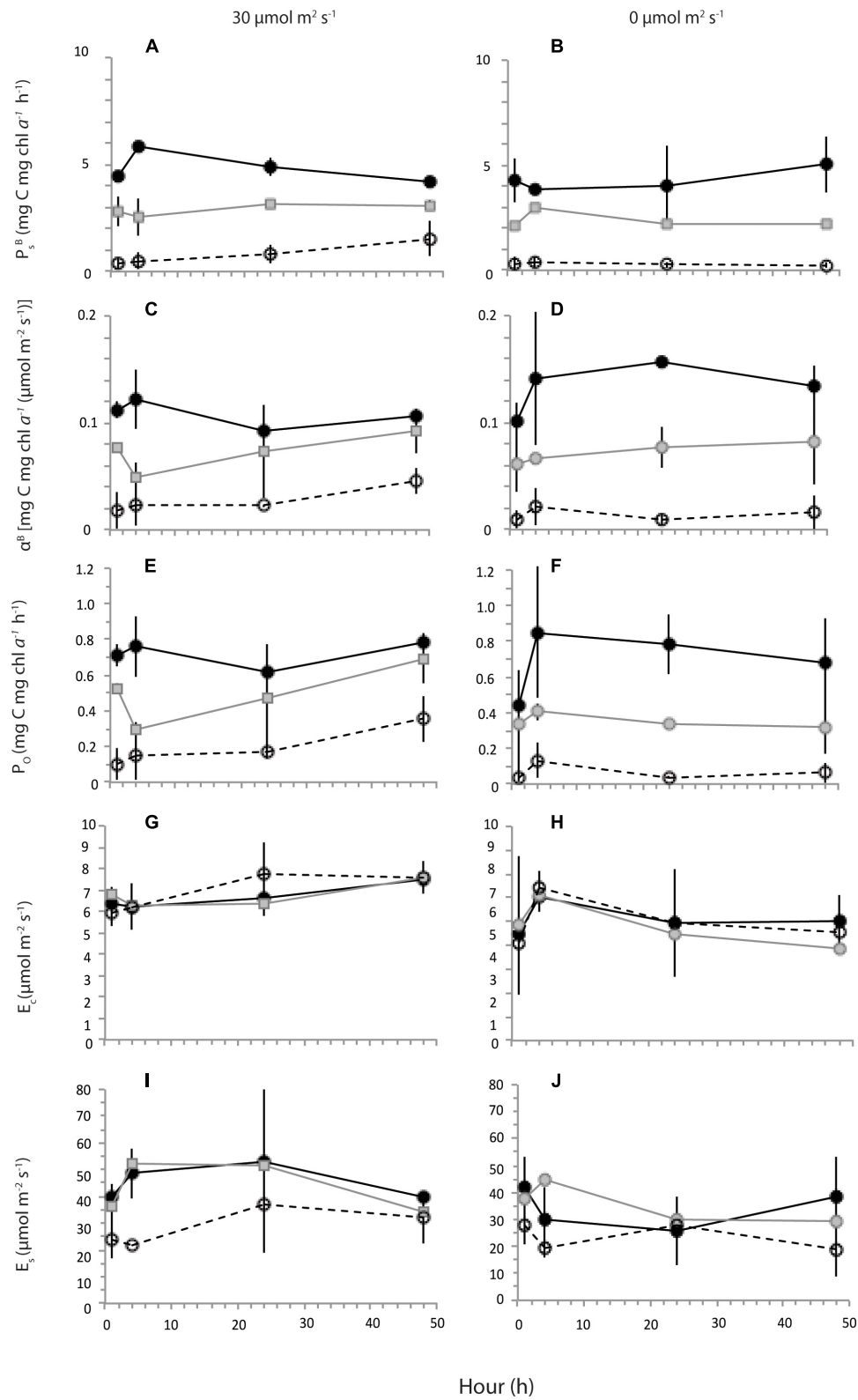
FIGURE 5 | Average (n = 2) photosynthetic parameters (see text for definitions) with standard deviation of algae grown in treatments of 30 (black), 20 (gray) and 12 (white) salinities for time intervals 1, 4, 24, and 48 h under 30 μmol m^{-2} s^{-1} **(A,C,E,G,I)** or in the dark **(B,D,F,H,J)**.

no significant difference in ice algal net production (relative to chl *a*) was found between samples melted with or without the addition of naturally derived filtered seawater. However, Baltic Sea surface water salinities can range from 2 to 24 (Leppäkoski et al., 2002), much lower than in this study (**Table 1**). It is possible that brackish waters of the Baltic Sea minimized a melt-processing effect due to acclimation of the local ice algal community to fresher *in situ* conditions. This suggestion supports conclusions by Rintala et al. (2014) that their results should only be directly applied to the Baltic Sea study region.

Rintala et al. (2014) also advocated for rapid ice melt overnight at room temperature versus at 4°C for 36 h, despite lower net production and chl *a*, as it was believed to limit algal growth during melting. In this research, we found that under conditions of stable temperature around the melting point of sea ice, faster ice melt was associated with greater maximum production (P^B_S). However, algal growth was not a factor in this study, as chl *a* was greater in FSW_{8:1} and FSW_{3:1} samples with shorter melt times, respectively. The Baltic Sea was also dominated by flagellated species (Rintala et al., 2014), while the ice algal community of Dease Strait was almost exclusively diatoms during this late-spring study period (Campbell et al., 2018). Differences in community composition could have contributed to variable responses between the studies, as individual species of algae are known to exhibit varying salinity tolerances (Ryan et al., 2004; Søgaard et al., 2011). Indeed, Balzano et al. (2011) showed that even different strains of the same marine diatom can exhibit varying sensitivities to decreases in salinity, where *Skeletonema marinoi* sourced from the moderately saline (7.5) North Sea exhibited greater sensitivity to experimental freshening than *S. marinoi* from the more brackish (2.5) conditions of the Baltic Sea. Similar to this study of sea ice in Dease Strait, algal blooms at the ice-ocean interface across the Arctic are typically characterized by diatoms like *N. frigida* growing at surface water salinities around 30 (Brandon et al., 2010; Poulin et al., 2011). As a result, the negative impact of unbuffered sample melt on algal photophysiology that we observed is likely more representative of bottom-ice algal communities in the Arctic than studies on non-diatom functional groups, or indeed algae from brackish environments.

Response of *Nitzschia frigida* Cultures to Experimental Treatments
Photosynthetic Responses of Algal Cultures
Variability in production between the melt treatments of Dease Strait samples as a result of time and/or salinity may have been driven by one or a combination of factors that include (i) optimal salinity ranges for growth and production (Arrigo and Sullivan, 1992), (ii) cell death or stress associated with melt time, darkness, and processing (Mikkelson and Witkowski, 2010; Rintala et al., 2014), (iii) inorganic nutrient (Rintala et al., 2014) and organic matter availability (Vähätalo and Järvinen, 2007), and (iv) the concentration of DIC (Rintala et al.,

2014). The relationship between photophysiological parameters and final sample salinity suggested that the change in salinity was a key factor in the difference between the three melt methods, but the field-based sample melt experiments employed in this study did not distinguish between salinity and other possible mechanisms. The lab experiments were designed to determine whether changes in salinity alone, or in combination with darkness, could produce changes in photophysiological parameters that were comparable to those seen in the field samples. The time duration for any changes in photophysiology to occur were also assessed.
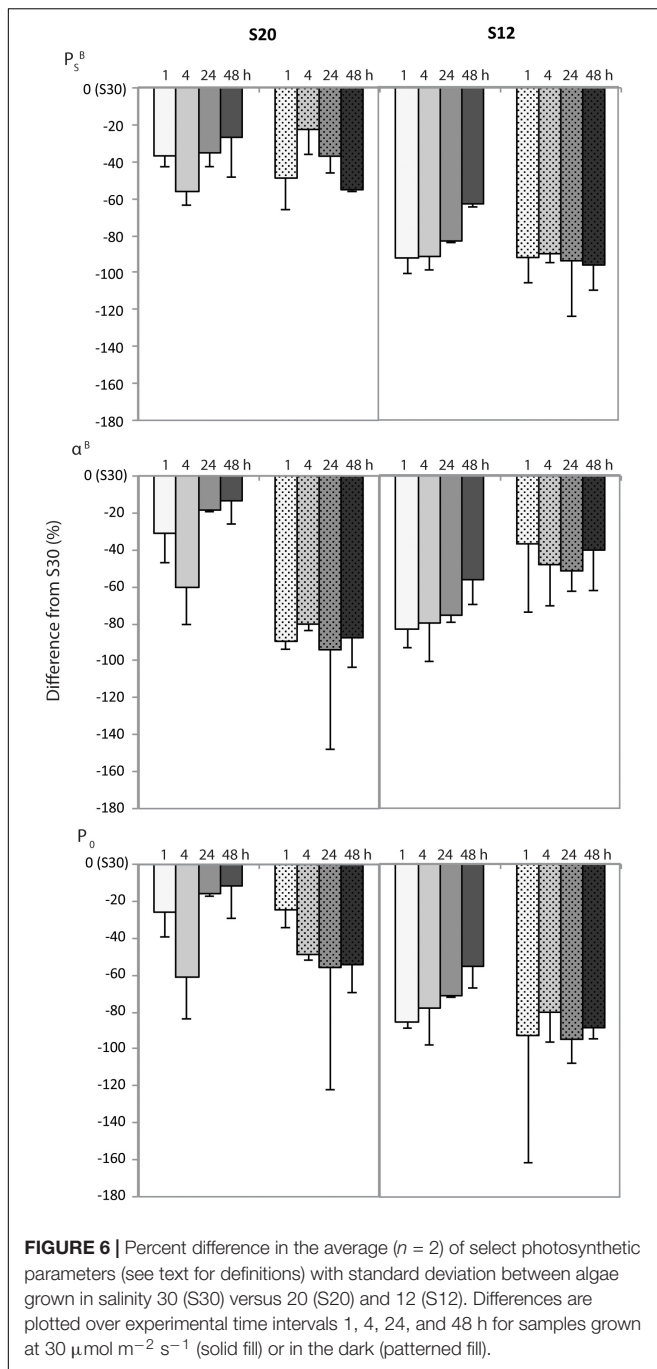
The similarity of our experimental results to the field observations supports our hypothesis that the photophysiology of sea ice algae is affected by sample melt procedure. The experimental results indicate that decreasing salinity alone caused the greatest observed changes in P^B_s, α^B, and P_0. Similar to the field observations, E_c and E_s did not change between treatments. While darkness enhanced the effects on P^B_s, α^B, and P_0, and there were temporal trends in some parameters, these impacts were comparatively minor relative to the salinity effects. In addition, given that the concentration of nutrients were consistent in all lab treatments, we note that photophysiological changes similar to those seen in the field samples can occur due to changes in salinity independent of nutrients.

Influence of Salinity in Driving Photosynthetic Responses of Algal Cultures
Previous studies have found that ice algal growth is optimized at salinities between 30 and 50 (Arrigo and Sullivan, 1992; Søgaard et al., 2011), while cells can survive under more extreme conditions between 10 and 60 with reduced metabolism (Grant and Horner, 1976; Vargo et al., 1986; Kottmeier and Sullivan, 1988). In particular, hypoosmotic (low salinity) conditions are thought to have a greater impact on ice algal cell functioning than hyperosmotic (high salinity) conditions due to cumulative impacts of osmotic stress following water uptake, salt stress with release of ions, and changes to the ion permeability of cell membranes (Kirst, 1990). These insights may thus in part explain the greater P^B_s and α^B in S30 and S20 laboratory samples as they were closest to the optimal salinity range described above. In comparison, the S12 laboratory sample was farthest from this range and had the lowest measurements of P^B_s, α^B, and P_0. By contrast, the consistently low values of photophysiological parameters, combined with low Fv/Fm and decreasing chlorophyll concentration, suggest that the cells in the S12 treatment were highly stressed, and probably dying.

Influence of Exposure Time on Photosynthetic Response of Algal Cultures
Longer melt times can promote gradual changes in salinity that limit the extent of osmotic shock to cells (Mikkelson and Witkowski, 2010), although, sea ice algae can take days to weeks to fully acclimate to altered growth salinities (Grant and Horner, 1976; Vargo et al., 1986). As a result, it is possible that the near-immediate changes to growth salinity during culture

FIGURE 6 | Percent difference in the average ($n = 2$) of select photosynthetic parameters (see text for definitions) with standard deviation between algae grown in salinity 30 (S30) versus 20 (S20) and 12 (S12). Differences are plotted over experimental time intervals 1, 4, 24, and 48 h for samples grown at 30 μmol m^{-2} s^{-1} (solid fill) or in the dark (patterned fill).

experiment was too short to assess whether these algae would have fully recovered from the initial salinity shock; however, our results demonstrate that the ability of cells to recover from hypoosmotic shock was likely hindered in the absence of photosynthesis. That is, ice algae did not acclimate to changes in salinity as well when in darkness, and in some instances, their photophysiological response actually continued to decline (e.g., P_0 at S20).

Greater differences in P^B_s, α^B, and P_0 parameters between light and dark experimental conditions in the S12 sample (**Figure 6** and **Supplementary Table S3**) supports that the combination of low light intensity and hypoosmotic stress was detrimental to algal production, more so than the impact of darkness alone. This finding contradicts the light dependency of ice algal photosynthetic responses to low salinity stress documented by Ralph et al. (2007) but could highlight the cause of exceptionally low production in regions of thick snow (low light) and low surface salinity, like Greenland fjords (Rysgaard et al., 2001; Søgaard et al., 2010; Leu et al., 2015). Future studies should investigate the potential for such additive responses of sea ice algae to their growth environments.

Influence of Dissolved Inorganic Carbon (DIC) Availability on Photosynthetic Response of Algal Cultures

Greater inventories of DIC may stimulate algal photosynthesis in carbon-limited systems (Riebesell et al., 1993), although this influence is not certain, as other studies have also documented a negligible impact on production (Hoppe et al., 2018). DIC was not constant across our experimental treatments and instead increased with the salinity of growth media. The higher concentrations of DIC calculated for S30 and S20 treatments, in comparison to S12, could have thus contributed to the measurement of greater production with salinity. However, recent studies on Arctic phytoplankton have also shown that production of particulate carbon following increased supply of DIC is time-dependent and requires a generation or more before the impact is pronounced (Schulz et al., 2013). Given the short-term (< 4 h) and arguably severe nature of responses to altered growth conditions in this study, we maintain that hypoosmotic shock was still a significant factor in driving variability in production response.

Drivers of Algal Response in Dease Strait Sea Ice

The majority of ice algae in Dease Strait were concentrated in the bottommost centimeter of the sea ice, suggesting that the majority of algae in this study were acclimated to the salinity of interface water infiltrating the skeletal layer. The scrape method of collecting FSW$_{8:1}$ samples produced melt water salinities most similar to interface water, limiting osmotic shock as detailed by our laboratory experiments. The scrape method also had the shortest duration of melt (< 4 h), which reduces the duration of exposure to any additive effects salinity stress and darkness may have had. We note that limiting melt duration

experiments produced more severe responses than field-based melt treatments that had more gradual exposure times (4–48 h). Nevertheless, the documented differences in P^B_s, α^B, and P_0 between salinity treatments within 4 h of exposure support a measurable impact of salinity on algal photophysiology that was quite rapid. Further calculation of the percent difference in these parameters at S20 and S12 from the reference values at S30 also indicates that after an initial 4 h shock period, algal photophysiology of illuminated samples become more similar to the S30 treatment (**Figure 6**). The duration of this

likely reduces the potential impact of predation (Rintala et al., 2014), although aquatic grazers were not explicitly observed in samples following taxonomic analysis (Campbell et al., 2018). In comparison, we attribute the lower estimates of P^B_s, α^B, and P_0 of $FSW_{3:1}$ and FSW_{zero} samples to greater levels of hypoosmotic shock. Based on these results it is our recommendation that bottom- ice samples be melted in filtered seawater volumes at minimum four times the volume of ice collected. Despite the number of perceived benefits to short melt times associated with the scrape treatment we believe that further work is required to ascertain an optimal duration of melt for ice samples, as shorter melt times could feasibly limit the potential for gradual acclimation of algae back-to true *in situ* levels of production and photophysiology. Algal photophysiology in S30 and S20 laboratory treatments varied little between zero and 30 μmol m^2 s^{-1} light intensities. However, for ease of sampling we also suggest the diluted ice melt should be undertaken in darkness versus at low light intensities that would be characteristic of conditions at the growth interface.

Although nutrients were controlled for during laboratory experiments, it is possible that the magnitude of variability in photophysiological response between field-based melt treatments was enhanced by additions of nutrients, organic constituents and DIC within the filtered seawater (Rintala et al., 2014). The average phosphate (PO_4), nitrate + nitrite ($NO_2 + NO_3$), and silicic acid ($Si(OH)_4$) in filtered seawater generated from Dease Strait was comparable to interface and bulk-ice estimates, where the concentration of nitrate + nitrite was found to be a limiting factor of algal production throughout the spring (Campbell et al., 2016). Due to low nitrogen concentrations in the region, it is thus unlikely that the addition of filtered seawater substantially increased ice algal production via enhanced nitrogen supply.

SUMMARY AND CONCLUSION

The photophysiological responses of ice algae were investigated following three possible methods of sample melt: (i) $\leq$ 4 h melt of the bottommost (< 1 cm) ice in a large volume of filtered seawater, (ii) 24 h melt of the bottom 5 cm ice section with moderate dilution of filtered seawater, and (iii) 48 h melt of the bottom 5 cm section with no filtered seawater dilution. Our field-based measurements clearly demonstrate that sample melting procedure affects the magnitude of many photophysiological parameters subsequently measured on the incubated meltwater. Lab experiments indicated that the differences observed between melting procedures can be primarily attributed to different levels of hypoosmotic stress. Of particular significance for estimates of primary production were decreases in P^B_S, α^B and P_0 in response to hypoosmotic stress experienced during unbuffered melt treatments with final salinities of approximately 10.

Based on the average intensity of PAR available to bottom-ice algae and photophysiological parameters calculated in this study, we estimate that the differences in production between melt procedures may account for between 7 and 64% of production variability in the Arctic. That is, the percent difference in production between melt treatments in this study over a possible range in ice algal production of 0.01 to 5.2 mg C mg chl a^{-1} h^{-1} across the Arctic (Arrigo et al., 2010) is 1–1.5 orders of magnitude. This exercise emphasizes that in addition to environmental controls driving variability in ice algal production around the Arctic (Leu et al., 2015), differences in sample melt methodology can impact calculations of production by over an order of magnitude. In turn, the approach chosen by scientists to melt ice samples almost certainly contributes to the variability in production reported across the Arctic.

Standardization of melt procedures in studies of sea ice production would help reduce uncertainty of method-related error. However, rather than adopting one single protocol for sample melt across the discipline, we advocate that efforts to replicate *in situ* conditions should be made as much as possible. The strong influence of salinity documented in this research indicates that maintaining salinity conditions is of particular importance for accurate production estimates, especially given that ice algae appear to rapidly respond to changes in salinity within a 4 h time period. Following this rationale, ice samples with organisms predominantly inhabiting the brine network prior to spring melt (e.g., upper ice profile), should be melted at higher salinities than those readily exposed to ocean surface waters (e.g., skeletal layer).

AUTHOR CONTRIBUTIONS

This work was led by KC and is based on the scientific design of KC, CJM, SR, and AJ. All co-authors provided in-field and/or laboratory-based support, as well as input during the composition and editing of the manuscript that was written by KC.

FUNDING

University of Manitoba. This paper is a contribution to SCOR Working Group 152 - Measuring Essential Climate Variables in Sea Ice (ECV-Ice).

for their support during laboratory experiments. Underlying data to support conclusions in this work are provided in the paper or Supplementary Information.

SUPPLEMENTARY MATERIAL

The Supplementary Material for this article can be found online at: https://www.frontiersin.org/articles/10.3389/feart.2019.00021/full#supplementary-material

REFERENCES

Arrigo, K. R., Mills, M. M., Kropuenske, L. R., van Dijken, G. L., Alderkamp, A. C., and Robinson, D. H. (2010). Photophysiology in two major Southern Ocean phytoplankton taxa: photosynthesis and growth of *Phaeocystis antarctica* and *Fragilariopsis cylindrus* under different irradiance levels. *Integr. Comp. Biol.* 50, 950–966. doi: 10.1093/icb/icq021

Arrigo, K. R., and Sullivan, C. W. (1992). The influence of salinity and temperature covariation on the photophysiological characteristics of Antarctic sea ice microalgae. *J. Phycol.* 28, 746–756. doi: 10.1111/j.0022-3646.1992.00746.x

Arrigo, K. R., Worthen, D. L., Lizotte, M. P., Dixon, P., and Dieckmann, G. (1997). Primary production in Antarctic sea ice. *Science* 276, 394–397. doi: 10.1126/science.276.5311.394

Aumack, C. F., and Juhl, A. R. (2015). Light and nutrient effects on the settling characteristics of the sea ice diatom Nitzschia frigida. *Limnol. Oceanog.* 60, 765–776. doi: 10.1002/lno.10054

Aumack, C. F., Juhl, A. R., and Krembs, C. (2014). Diatom vertical migration within land-fast Arctic sea ice. *J. Mar. Syst.* 139, 496–504. doi: 10.1016/j.jmarsys.2014.08.013

Babin, M., Morel, A., and Gagnon, R. (1994). An incubator designed for extensive and sensitive measurements of phytoplankton photosynthetic parameters. *Limnol. Oceanog.* 39, 694–702. doi: 10.4319/lo.1994.39.3.0694

Balzano, S., Sarno, D., Wiebe, H. C., and Kooistra, F. (2011). Eggects of salinity on the growth rate and morphology of ten Skeletonema strains. *J. Plank. Res.* 33, 937–945. doi: 10.1093/plankt/fbq150

Bates, S. S., and Cota, G. F. (1986). Fluorescence induction and photosynthetic responses of Arctic ice algae to sample treatment and salinity. *J. Phycol.* 22, 421–429. doi: 10.1111/j.1529-8817.1986.tb02484.x

Bergmann, M. A., Welch, H. E., Butler-Walker, J. E., and Siferd, T. D. (1991). Ice algal photosynthesis at resolute and saqvaqjuac in the Canadian Arctic. *J. Mar. Syst.* 2, 43–52. doi: 10.1016/0924-7963(91)90012-J

Brandon, M. A., Cottier, F. R., and Nilsen, F. (2010). "Chapter 3: sea ice and oceanography," in *Sea Ice*, eds D. N. Thomas and G. S. Dieckmann (Hoboken, NJ: Wiley-Blackwell), 97–130.

Brown, K. A., Miller, L., Mundy, C. J., Francois, R., Gosselin, M., Carnat, G., et al. (2015). Inorganic carbon system dynamics in landfast Arctic sea ice during the early-melt period. *J. Geophys. Res. Oceans* 120, 3542–3566. doi: 10.1002/2014JC01062

Campbell, K., Mundy, C. J., Belzile, C., Delaforge, A., and Rysgaard, S. (2018). Seasonal dynamics of algal and bacterial communities in Arctic sea ice under variable snow cover. *Polar Biol.* 41, 41–58. doi: 10.1007/s00300-017-2168-2

Campbell, K., Mundy, C. J., Gosselin, M., Landy, J. C., Delaforge, A., and Rysgaard, S. (2017). Net community production in the bottom of first-year sea ice over the Arctic spring bloom. *Geophys. Res. Lett.* 44, 8971–8978. doi: 10.1002/2017GL074602

Campbell, K., Mundy, C. J., Landy, J. C., Delaforge, A., Michel, C., and Rysgaard, S. (2016). Community dynamics of bottom-ice algae in Dease Strait of the Canadian Arctic. *Prog. Oceanog.* 149, 27–39. doi: 10.1016/j.pocean.2016.10.005

Cota, G., and Smith, R. E. H. (1991). Ecology of bottom ice algae: III. Comparative physiology. *J. Mar. Syst.* 2, 297–315. doi: 10.1016/0924-7963(91)90038-V

Cota, G. F., and Horne, E. P. W. (1989). Physical control of arctic ice algal production. *Mar. Ecol. Prog. Ser.* 52, 111–121. doi: 10.3354/meps052111

Fernandez-Mendez, M., Olsen, L. M., Kauko, H. M., Meyer, A., Rosel, A., Merkouriadi, I., et al. (2018). Algal hot spots in a changing arctic ocean: sea-ice

ridges and the snow-ice interface. *Front. Mar. Sci.* 5:75. doi: 10.3389/fmars.2018.00075

Garrison, D. L., and Buck, K. R. (1986). Organism losses during ice melting: a serious bias in sea ice community studies. *Polar Biol.* 6, 237–239. doi: 10.1007/BF00443401

Gosselin, M., Legendre, L., Therriault, J.-C., and Demers, S. (1990). Light and nutrient limitation of sea-ice microalgae (Hudson Bay, Canadian Arctic). *J. Phycol.* 26, 220–232. doi: 10.1111/j.0022-3646.1990.00220.x

Gosselin, M., Levasseur, M., Patricia, A. W., Horner, R. A., and Booth, B. C. (1997). New measurements of phytoplankton and ice algal production in the Arctic Ocean. *Deep Sea Res.* 44, 1623–1644. doi: 10.1016/S0967-0645(97)00054-4

Grant, W. S., and Horner, R. A. (1976). Growth responses to salinity variation in four Arctic ice diatoms. *J. Phycol.* 261, 180–185. doi: 10.1111/j.1529-8817.1976.tb00498.x

Grasshoff, K., Ehrhardt, M., and Kremling, K. (1983). *Methods of Seawater Analysis*. Weinheim: Chemie.

Guillard, R. R. L., and Hargraves, P. E. (1993). *Stichochrysis* immobilis is a diatom, not a chrysophyte. *Phycolog.* 32, 234–236. doi: 10.2216/i0031-8884-32-3-234.1

Hegseth, E. N. (1998). Primary production of the northern Barents Sea (1998). *Polar Res.* 17, 113–123. doi: 10.1111/j.1751-8369.1998.tb00266.x

Holm-Hansen, O., Lorenzen, C. J., Holmes, R. W., and Strickland, J. D. H. (1965). Fluorometric Determination of Chlorophyll. *ICES J. Mar. Sci.* 30, 3–15. doi: 10.1093/icesjms/30.1.3

Hoppe, C. J. M., Wolf, K. E. K., Schuback, N., Tortell, P. D., and Rost, B. (2018). Compensation of ocean acidification effects in Arctic phytoplankton assemblages. *Nat. Clim. Change* 8, 529–533. doi: 10.1038/s41558-018-0142-9

Johnsen, G., and Hegseth, E. N. (1991). Photoadaptation of sea-ice microalgae in the Barents Sea. *Polar Biol.* 11, 179–184. doi: 10.1007/BF00240206

Juhl, A. R., and Krembs, C. (2010). Effects of snow removal and algal photoacclimation on growth and export of ice algae. *Polar Biol.* 33, 1057–1065. doi: 10.1007/s00300-010-0784-1

Kaartokallio, H., Kuosa, H., Thomas, D. N., Granskog, M. A., and Kivi, K. (2007). Biomass, composition and activity of organism assemblages along a salinity gradient in sea ice subjected to river discharge in the Baltic Sea. *Polar Biol.* 30, 183–197. doi: 10.1007/s00300-006-0172-z

Kirst, G. O. (1990). Salinity tolerance of eukaryotic marine algae. *Ann. Rev. Plant Physiol. Plant Mol. Biol.* 42, 21–53. doi: 10.1146/annurev.pp.41.060190.000321

Kottmeier, S. T., and Sullivan, C. W. (1988). Sea ice microbial communities (SIMCO). effects of temperature and salinity on rates of metabolism and growth of autotrophs and heterotrophs. *Polar Biol.* 8, 293–304. doi: 10.1007/BF00263178

Kuhl, M., Glud, R. N., Borum, J., Roberts, R., and Rysgaard, S. (2001). Photosynthetic performance of surface-associated algae below sea ice as measured with a pulse-amplitude-modulated (PAM) fluorometer and O2 microsensors. *Mar. Ecol. Progr. Ser.* 223, 1–14. doi: 10.3354/meps223001

Lange, B. A., Flores, H., Michel, C., Beckers, J. F., Bublitz, A., Casey, J. A., et al. (2017). Pan-Arctic sea ice-algal chl a biomass and suitable habitat are largely underestimated for multi-year ice. *Glob. Change Biol.* 23, 4581–4597. doi: 10.1111/gcb.13742

Leeuwe, M. V., Tedesco, L., Arrigo, K. R., Assmy, P., Campbell, K., Meiners, K. M., et al. (2018). Microalgal community structure and primary production in Arctic and Antarctic sea ice: a synthesis. *Elem. Sci. Anth.* 6:25. doi: 10.1525/elementa.267

Legendre, L., Ackley, S. F., Dieckmann, G. S., Gullicksen, B., Horner, R., Hoshiai, T., et al. (1992). Ecology of sea ice biota: part 2, global significance. *Polar Biol.* 12, 429–444. doi: 10.1007/BF00243113

Legendre, L., Demers, S., Yentsch, C. M., and Yentsch, C. S. (1983). The 14C method: patterns of dark CO2 fixation and DCMU correction to replace the dark bottle. *Limnol. Oceanog.* 28, 996–1003. doi: 10.4319/lo.1983.28.5.0996

Leppäkoski, E., Gollasch, S., and Olenin, S. (2002). *Invasive Aquatic Species of Europe. Distribution, Impacts and Management.* Dordrecht: Kluwer. doi: 10.1007/978-94-015-9956-6

Leu, E., Mundy, C. J., Assmy, P., Campbell, K., Gabrielsen, T. M., Gosselin, M., et al. (2015). Arctic spring awakening – steering principles behind the phenology of vernal ice algae blooms. *Prog. Oceano.* 139, 151–170. doi: 10.1016/j.pocean.2015.07.012

Leu, E., Soreide, J. E., Hessen, D. O., Falk-Peterson, S., and Berge, J. (2011). Consequences of changing sea-ice cover for primary and secondary producers in the European Arctic shelf seas: timing, quantity, and quality. *Prog. Oceanog.* 90, 18–32. doi: 10.1016/j.pocean.2011.02.004

Maxwell, K., and Johnson, G. N. (2000). Chlorophyll fluorescence—a practical guide. *J. Exp. Bot.* 51, 659–668. doi: 10.1093/jexbot/51.345.659

McMinn, A., Ashworth, C., and Ryan, K. G. (2000). In situ net primary productivity of an Antarctic fast ice bottom algal community. *Aquat. Microb. Ecol.* 21, 177–185. doi: 10.3354/ame021177

McMinn, A., and Hegseth, E. N. (2007). Sea ice primary productivity in the northern Barents Sea, spring 2004. *Polar Biol.* 30, 289–294. doi: 10.1007/s00300-006-0182-x

McMinn, A., Muller, M. N., Martin, A., and Ryan, K. G. (2014). The response of antarctic sea ice algae to changes in pH and CO2. *PLoS One* 9:e86984. doi: 10.1371/journal.pone.0086984

McMinn, A., Skerrstt, J., Trull, T., Ashworth, C., and Lizotte, M. (1999). Nutrient stress gradient in the bottom 5 cm of fast ice, McMurdo Sound, Antarctica. *Polar Biol.* 21, 220–227. doi: 10.1007/s003000050

Michel, C., Legendre, L., Demers, S., and Therriault, J.-C. (1988). Photoadaptation of sea-ice microalgae in springtime: photosynthesis and carboxylating enzymes. *Mar. Ecol. Prog. Ser.* 50, 177–185. doi: 10.3354/meps050177

Mikkelson, D. M., and Witkowski, A. (2010). Melting sea ice for taxonomic analysis: a comparison of four melting procedures. *Polar Res.* 29, 451–454. doi: 10.1111/j.1751-8369.2010.00162.x

Miller, L. A., Fripiat, F., Else, B. G. T., Bowman, J. S., Brown, K. A., Collins, R. E., et al. (2015). Methods for biogeochemical studies of sea ice: the state of the art, caveats, and recommendations. *Elem. Sci. Anth.* 3:38. doi: 10.12952/journal.elementa.000038

Mock, T., and Gradinger, R. (1999). Determination of Arctic ice algal production with a new in situ incubation technicrue. *Mar. Ecol. Prog. Ser.* 177, 15–26. doi: 10.3354/meps177015

Norrman, B., and Anderson, A. (1994). Developement of ice biota in temperate sea area (Gulf of Bothnia). *Polar Biol.* 14, 531–537. doi: 10.1007/BF00238222

Parkhill, J., Maillet, G., and Cullen, J. J. (2001). Fluorescence-based maximum quantum yield for PSII as a diagnostic for nutrient stress. *J. Phycol.* 37, 517–529. doi: 10.1046/j.1529-8817.2001.037004517.x

Parsons, T. R., Maita, Y., and Lalli, C. M. (1984). *Manual of Chemical and Biological Methods for Seawater Analysis.* New York, NY: Pergamon Press.

Platt, T., Gallegos, C. L., and Harrison, W. G. (1980). Photoinhibition of photosynthesis in natural assemblages of marine phytoplanton. *J. Mar. Res.* 38, 687–701.

Poulin, M., Daugbjerg, N., Gradinger, R., Ilyash, L., Ratkova, T., and Quillf, C. (2011). The pan-Arctic biodiversity of marine pelagic and sea-ice unicellular eukaryotes: a first-attempt assessment. *Mar. Biodiv.* 41, 13–28. doi: 10.1007/s12526-010-0058-8

Ralph, P. J., Ryan, K. G., Martin, A., and Fenton, G. (2007). Melting out of sea ice causes greater photosynthetic stress in algae than freezing in. *J. Phycol.* 43, 948–956. doi: 10.1111/j.1529-8817.2007.00382.x

Riebesell, U., Wolf- Gladrow, D. A., and Smetacek, V. (1993). Carbon dioxide limitation of marine phytoplankton growth rates. *Nature* 361, 249–251. doi: 10.1038/361249a0

Rintala, J.-M., Piiparinen, J., Blomster, J., Majaneva, M., Muller, S., Uusikivi, J., et al. (2014). Fast direct melting of brackish sea-ice samples results in biologically more accurate results than slow buffered melti. *Polar Biol.* 37, 1811–1822. doi: 10.1007/s00300-014-1563-1

Różańska, M., Gosselin, M., Poulin, M., Wiktor, J. M., and Michel, C. (2009). Influence of environmental factors on the development of bottom ice protist communities during the winter-spring transition. *Mar. Ecol. Prog. Ser.* 386, 43–59. doi: 10.3354/meps08092

Ryan, K. G., Ralph, P., and McMinn, A. (2004). Acclimation of Antarctic bottom-ice algal communities to lowered salinities during melting. *Polar Biol.* 27, 679–686. doi: 10.1007/s00300-004-0636-y

Rysgaard, S., Kuhl, M., Glud, R. N., and Hansen, J. W. (2001). Biomass, production and horizontal patchiness of sea ice algae in a high-Arctic fjord (Young Sound, NE Greenland). *Mar. Ecol. Prog. Ser.* 223, 15–26. doi: 10.3354/meps223015

Schulz, K. G., Bellerby, R. G. J., Brussaard, C. P. D., Büdenbender, J., Czerny, J., Engel, A., et al. (2013). Temporal biomass dynamics of an Arctic plankton bloom in response to increasing levels of atmospheric carbon dioxide. *Biogeosci.* 10, 161–180. doi: 10.5194/bg-10-161-2013

Simmonds, I. (2015). Comparing and contrasting the behaviour of Arctic and Antarctic sea ice over the 35 year period 1979–2013. *Ann. Glaciol.* 56, 18–28. doi: 10.3189/2015AoG69A909

Smith, R. E., Harrison, W. G., Harris, L. R., and Herman, A. W. (1990). Vertical fine structure of particulate matter and nutrients in sea ice of the high Arctic. *Can. J. Fish. Aquat. Sci.* 47, 1348–1355. doi: 10.1139/f90-154

Smith, R. E. H., Anning, J., Clement, P., and Cota, G. (1988). Abundance and production of ice algae in resolute passage, Canadaian Arctic. *Mar. Ecol. Prog. Ser.* 48, 251–263. doi: 10.3354/meps048251

Søgaard, D. H., Hansen, P. J., Rysgaard, S., and Glud, R. N. (2011). Growth limitation of three Arctic sea ice algal species: effects of salinity, pH, and inorganic carbon availability. *Polar Biol.* 34, 1157–1165. doi: 10.1007/s00300-011-0976-3

Søgaard, D. H., Kristensen, M., Rysgaard, S., Glud, R. N., Hansen, P. J., and Hilligsoe, K. M. (2010). Autotrophic and heterotrophic activity in Arctic first-year sea ice: seasonal study from Malene Bight, SW Greenland. *Mar. Ecol. Prog. Ser.* 419, 31–45. doi: 10.3354/meps08845

Strickland, J. D. H., and Parsons, T. R. (1972). *A Practical Handbook of Seawater Analysis.* Ottawa: Fisheries Board of Canada.

Subba Rao, D. V., and Platt, T. (1984). Primary production of arctic waters. *Polar Biol.* 3, 191–201. doi: 10.1007/BF00292623

Suzuki, Y., Kudoh, S., and Takahashi, M. (1997). Photosynthetic and respiratory characteristics of an Arctic ice algal community living in low light and low temperature conditions. *J. Mar. Syst.* 11, 111–121. doi: 10.1016/S0924-7963(96)00032-2

Thomas, D. N., Papadimitriou, S., and Michel, C. (2010). "Chapter 12: biogeochemistry of sea ice," in *Sea Ice*, eds D. N. Thomas and G. S. Dieckmann (Hoboken, NJ: Wiley-Blackwell), 425–468.

Vähätalo, A. V., and Järvinen, M. (2007). Photochemically produced bioavailable nitrogen from biologically recalcitrant dissolved organic matter stimulates production of a nitrogen-limited microbial food web in the Baltic Sea. *Limnol. Oceang.* 52, 132–143. doi: 10.4319/lo.2007.52.1.0132

Vargo, G. A., Fanning, K., Heil, C., and Bell, L. (1986). Growth rates and the salinity response of an Antarctic ice microflora community. *Polar Biol.* 5, 241–247. doi: 10.1007/BF00446092

Vihma, T. (2014). Effects of Arctic sea ice decline on weather and climate: a review. *Surv. Geophys.* 35, 1175–1214. doi: 10.1007/s10712-014-9284-0

Welch, H. E., and Bergmann, M. A. (1989). Seasonal development of ice algae and its prediction from environmental factors near resolute, NWT, Canada. *Can. J. Fish. Aquat. Sci.* 46, 1793–1804. doi: 10.1139/f89-227

Welch, H. E., Bergmann, M. A., Jorgenson, J. K., and Burton, W. (1988). A sub ice suction corer for sampling epontic ice algae. *Can. J. Fish. Aquat. Sci.* 45, 562–568. doi: 10.1139/f88-067